Astron. Astrophys. 116, 130–136 (1982)

ASTRONOMY AND ASTROPHYSICS

CO $J=3\rightarrow2$ and Submillimetre Continuum Observations of Two Molecular Outflow Sources

J. P. Phillips[1], Glenn J. White[2], P. A. R. Ade[2], C. T. Cunningham[2], K. J. Richardson[2], E. I. Robson[3], and Graeme D. Watt[4]

[1] Astronomy Division, Space Science Department of ESA, P.O. Box 299, 2200 AG Noordwijk zh, The Netherlands
[2] Department of Physics, Queen Mary College, Mile End Road, London E1 4NS, England
[3] Division of Physics and Astronomy, Preston Polytechnic, Corporation Street, Preston PR1 2TQ, England
[4] Department of Mathematics, UMIST, P.O. Box 88, Manchester M60 1QD, England

Received February 5, accepted August 20, 1982

Summary. We present CO $J=3\rightarrow2$ molecular line spectra, and submillimetre photometry at wavelengths $\lambda\lambda$377 μm, 811 μm, and 1136 μm for the sources L 1551 and IRC+10 216. Detailed analysis of the L 1551 spectra indicates the presence of strong velocity gradients in the CO emission zones, implying low optical depths and relatively high densities. The central source IRS 5 displays an infrared excess which cannot be explained in terms of a single temperature continuum. The emission zone is probably compact with respect to the instrumental beam size at the wavelength of peak emission ($\lambda\sim50$ μm), and may represent an accretion disc responsible for collimation of the high velocity gas. The far-infrared continuum of IRC+10 216 has been synthesised by assuming a distribution of optically thin grains whose emissivity varies as $\varepsilon\propto\lambda^{-1}$, and the CO $J=3\rightarrow2$ spectrum for this source supports earlier $J=2\rightarrow1$ observations, implying a variable mass-loss rate.

Key words: CO $J=3\rightarrow2$ – submillimetre photometry – stellar outflows

1. Introduction

Although L 1551 (IRS 5) and IRC+10 216 are both associated with relatively high velocity molecular outflows, it seems clear that we are witnessing quite disparate phenomena. Thus, in the case of L 1551 (IRS 5) it appears likely that the outflow takes the form of a stellar wind emanating from a newly formed or pre-main sequence star, and confined to jets by an accretion disc acting as a nozzle. This in turn appears to be interacting with a considerably more massive enveloping cloud, leading to microwave line profiles which display evidence for both post- and preshock components (Snell et al., 1980). In contrast, the outflow from IRC+10 216 has its genesis in a considerably later type star, appears symmetric, has a lower velocity of outflow, and is almost certainly powered by a different mechanism from that which characterises the mass-loss in L 1551.

In the following study, we present and discuss observations of these sources in the $J=3\rightarrow2$ transition of CO, and at wavelengths $\lambda=377$ μm, 811 μm, and 1136 μm in the far infrared. All results were obtained with the $3^{m}.8$ United Kingdom Infrared Telescope in Hawaii (UKIRT).

Send offprint requests to: J. P. Phillips

Table 1. Submillimetre continuum photometry

Source	Effective wavelength (μm)	Bandpass (GHz)	Flux (Jy)
L1551	377	420	107 ±8
L1551	811	140	15.0±3.0
IRC+10,216	377	420	35.2±6.6
IRC+10,216	811	140	9.8±1.6
IRC+10,216	1136	85	3.5±0.9

2. The Observations

The CO $J=3\rightarrow2$ (345 GHz) spectra were obtained with the QMC submillimetre and millimetre spectral line receivers during December 1980. The instrumental beamwidth was 1.'0, system noise temperature measured to be 420 K, and zenith optical depth was typically of order ~0.3. The spectra were calibrated in the usual way (White et al., 1979) to yield corrected antenna temperature T_A^*, and are estimated to be accurate to better than 15%. Absolute telescope pointing capability was measured using SAO stars and found to have an RMS value of order ~15″.

The continuum data (Table 1) were obtained with the QMC submillimetre photometer which has been described previously (Robson et al., 1978). For these observations three passbands were employed with mean frequencies 264 GHz (1136 μm), 370 GHz (811 μm), and 796 GHz (377 μm) with bandwidths of 85 GHz, 140 GHz, and 420 GHz, respectively. The detector was a ^{3}He cooled composite Ge bolometer with an electrical NEP of $3\,10^{-15}$ W Hz$^{-1/2}$. Calibration is primarily by comparison with the planet Mars for which we assume that the submillimetre emission is adequately described by the model of Wright (1976). For these observations a secondary calibration via Jupiter was used. The measured brightness temperature for Jupiter with respect to Mars through these passbands is given in Cunningham et al. (1981). The HPBW for all three channels was measured to be 86″. Offset guiding on SAO stars was used to define source positions.

3. L 1551

The dark cloud L 1551 is a nearby region of star formation characterised by substantial kinematic activity. Within its bound-

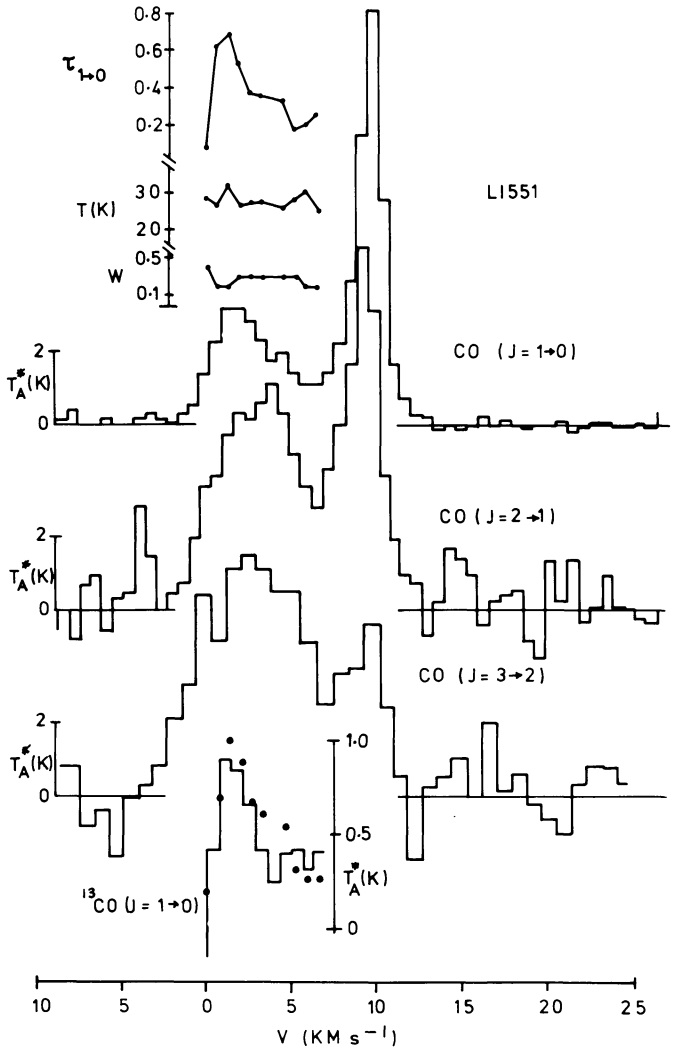

Fig. 1. $J=3\rightarrow2$ CO observations of L 1551 at α (1950) $=04^h28^m31^s.6$, $\delta(1950)=17°59'52''$. For comparison, we show CO $J=1\rightarrow0$, $J=2\rightarrow1$, and ^{13}CO $J=1\rightarrow0$ profiles obtained by Snell et al. (1980) with a comparable beamsize. The variation of dilution W, $J=1\rightarrow0$ CO optical depth $\tau_{1\rightarrow0}$ and gas kinetic temperature T are also given for the model described in the text, together with points for a synthesised ^{13}CO $J=1\rightarrow0$ spectrum

ary are contained several T-Tauri stars and Herbig-Haro objects, of which HH 28 and HH 29 are apparently receding (Cudworth and Herbig, 1979) from a centrally located source IRS 5 (Strom et al., 1976). This source in turn possesses a steep continuum in the near infrared (Beichman and Harris, 1981) which appears to peak at $\lambda\sim50\,\mu$m (Fridlund et al., 1980; see also later) and may represent a newly formed or forming early-type star shrouded by a high-extinction placental cloud.

The region was first mapped in the $J=1\rightarrow0$ transition of CO by Knapp et al. (1976) who found the line to consist of two principal components; a narrow spike feature at $V_{LSR}\sim7.5\,\mathrm{km\,s^{-1}}$, and a weaker but much broader "wing" component with $-5\,\mathrm{km\,s^{-1}}\lesssim V_{LSR}\lesssim+5\,\mathrm{km\,s^{-1}}$. Subsequent mapping by Snell et al. (1980) showed the wings to be confined within lobes orientated in a northeast-southwest direction, with the northeast lobe corresponding to a velocity range $10\,\mathrm{km\,s^{-1}}\lesssim V_{LSR}\lesssim20\,\mathrm{km\,s^{-1}}$.

Snell et al. (1980) hypothesize that the bipolar CO complex originates from the interaction of high velocity jets from IRS 5 with a circumstellar cloud. Their results further indicate that CO wing emission may be optically thin at several locations in this region.

In order to specify the properties of this CO cloud more clearly, we have taken $J=3\rightarrow2$ CO profiles at three locations in L 1551. Two of these spectra (one at least of which indicates optically thick emission) have been briefly discussed by White et al. (1981). We have also observed the optically thin zone near $\alpha(1950)=04^h28^m31^s.6$, $\delta(1980)=17°59'52''$, and our results are presented in Fig. 1.

In discussing their $J=1\rightarrow0$ results, Snell et al. (1980) were able to determine that kinetic temperatures in the line wing ranged between 8 K and 35 K. Our present results supplement this data (the beam-size for the present work is essentially the same as that of the lower frequency results), and enable tighter constraints on the physical conditions responsible for this emission.

Where local gas kinetic temperature T and the H_2 density n_{H_2} lead to thermalisation of the lower rotational energy states of CO, the observed antenna temperature will be given by

$$T_A^*(J+1\rightarrow J)=5.53(J+1)\left\{\frac{1}{e^{\frac{5.53(J+1)}{T}}-1}-\frac{1}{e^{\frac{5.53(J+1)}{T_{BB}}}-1}\right\}\cdot(1-e^{-\tau_{J+1\rightarrow J}})W, \quad (1a)$$

where

$$\tau_{J+1\rightarrow J}=\tau_{1\rightarrow0}(J+1)^2e^{-\frac{2.76J(J+1)}{T}}\frac{\left(1-e^{-\frac{5.53(J+1)}{T}}\right)}{\left(1-e^{-\frac{5.53}{T}}\right)}. \quad (1b)$$

W is dilution, τ is the optical depth, and J is the total angular momentum quantum number of the lower transition state.

The use of all three CO profiles in Fig. 1 in conjunction with Eq. (1) enables a least-squares solution to be calculated for W, T and $\tau_{1\rightarrow0}$. Results of this analysis for the wing feature are presented in Fig. 1. By further assuming a $|^{12}CO|/|^{13}CO|$ ratio of ~40 and employing the values T, W and $\tau_{1\rightarrow0}$ found above, it is possible to determine a ^{13}CO $J=1\rightarrow0$ profile which compares very favourably with observations (Snell et al., 1980).

Several interesting results ensue from such an analysis. First, the kinetic temperatures obtained are moderately high $T\sim25\rightarrow30$ K), and appear more or less constant over the velocity regime for which this parameter can be reliably evaluated. Similarly, the dilution W appears broadly invariant, having typical values $W\sim0.3$; a result which was not available to Snell et al. with their more limited data base. Finally, the CO line shape is seen to arise primarily from changes of optical depth; although $\tau_{1\rightarrow0}<1$, in the higher frequency transitions optical depth $\tau_{J+1\rightarrow J}(J>1)$ is significantly greater than unity – a factor responsible for the comparability of $J=3\rightarrow2$ and $J=2\rightarrow1$ line wing strengths.

Using the parameters discussed above, and assuming a uniform velocity gradient through the wing emission region, we may therefore determine a CO column density

$$N(CO)=\frac{2.85\,10^{14}\tau_{1\rightarrow0}\Delta V(\mathrm{km\,s^{-1}})T}{(1-e^{-5.53/T})}\sim2.8\,10^{16}\,\mathrm{cm^{-2}} \quad (2)$$

or, taking $|CO|/|H_2|\sim5\,10^{-5}$, this gives $N(H_2)\sim5.5\,10^{20}$. Adopting a local H_2 density $n(H_2)\gtrsim10^4\,\mathrm{cm^{-3}}$ (required for the

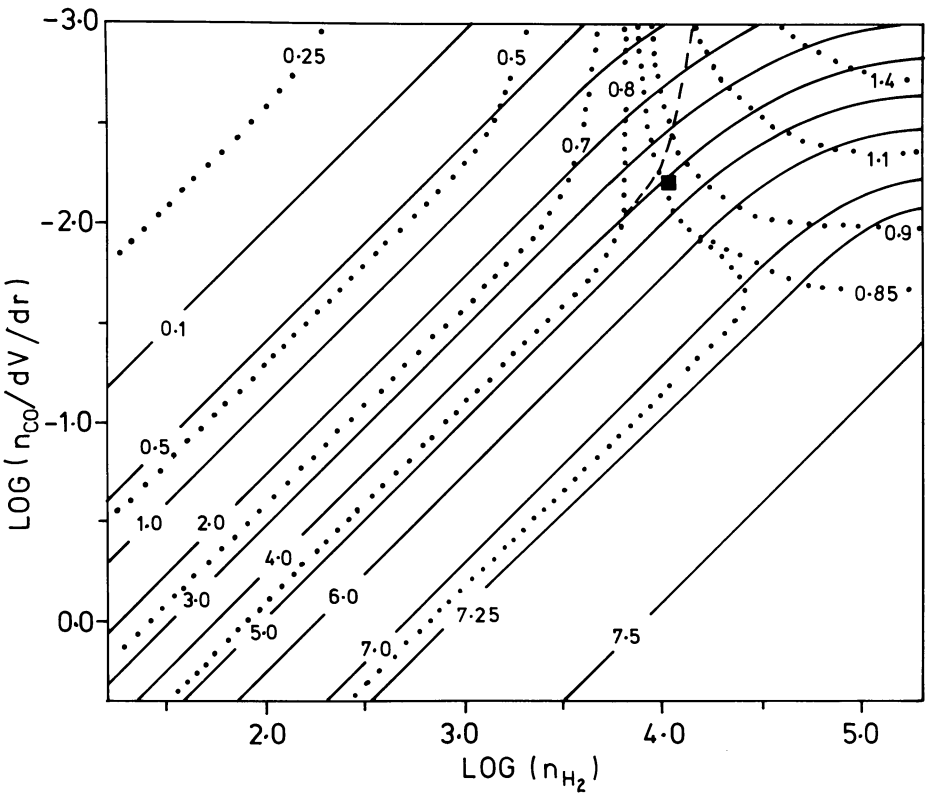

Fig. 2. LVG CO line modelling for the L 1551 spike feature ($T=14.3$ K). Dotted lines ($\cdots$) give ratios $T_A^*(J=2\rightarrow1)/T_A^*(J=3\rightarrow2)$, the dashed line (– – –) corresponds to $T_A^*(1\rightarrow0)/T_A^*(3\rightarrow2)=0.42$, as observed, and solid lines (———) represent constant $T_A^*(J=3\rightarrow2)$. The marker (■) locates the best fit solution to the observed line strengths

assumed level of CO thermalisation) implies a wing column depth $\Delta r \lesssim 0.081$ pc; considerably less than the overall size of the emission region (~ 0.5 pc). Such a result strongly suggests that the wing emission arises from warm, dense post-shock material, with low dilution W indicating substantial fragmentation in the post shock zone.

The spike component in contrast shows a strongly attenuated $J=3\rightarrow2$ line strength compared with lower frequency results, and it is instructive to briefly discuss possible causes for this behaviour.

If CO rotational levels are thermalised, the observed temperature ratio

$$\chi = T_A^*(J=3\rightarrow2)/T_A^*(J=1\rightarrow0) \sim 0.42$$

is obtained for $T \simeq 6.6$ K. Since, however, this implies (for $W \sim 1$) a value $T_A^*(J=1\rightarrow0) \sim 3.4$ K which is considerably less than observed, this explanation does not appear to be viable. Alternatively, a low ratio χ may originate if $\tau_{3\rightarrow2}/\tau_{1\rightarrow0} < 1$. Again, however, this can be shown to imply $T \lesssim 6.2$ K and unrealistically low line strengths.

It seems therefore clear that the observed range of spike temperatures reflects the influence of photon-trapping effects. Adopting from the observed $J=1\rightarrow0$ line strength a provisional gas kinetic temperature $T \sim 14.3$ K, we have employed an LVG analysis similar to that of Goldreich and Kwan (1974), using the CO collisional rates of Green and Thaddeus (1974) to obtain the contour map in Fig. 2. It is plain from this that an adequate fit to all three transition temperatures may be obtained. In particular, the analysis permits us to define unique values of $n_{H_2} \sim 6.8\ 10^3$ cm^3 and $dV/dr \sim 56$ km s^{-1} ps^{-1}, with an uncertainty of $\sim \pm 0.1$ dex in each value. Contour maps at higher values of gas temperature T have also been evaluated; we find that the values of n_{H_2}, dV/dr thus determined are relatively insensitive to T, and for $T \lesssim 25$ K (the highest temperature case analysed) are the same within errors as the values quoted for $T \simeq 14.3$ K. Therefore, although it is not possible to claim a significant temperature differential between spike and wing features, the present analysis would appear to imply that the spike derives from a zone with strong velocity gradients. From the observed spike full width at half maximum $\Delta V \sim 1.5$ km s^{-1} (obtained after deconvolving for instrumental frequency response), it is then possible to identify the spike as originating in a region of depth $\lesssim 2.7\ 10^{-2}$ pc. Column density $N(H_2) \sim 5.6\ 10^{20}$ cm^2 is comparable to that of the wing, and implies optical extinction $A_V \sim 0.5$ mag.

In achieving these results we have assumed that the $J=1\rightarrow0$, $J=2\rightarrow1$, and $J=3\rightarrow2$ lines peak at the same velocity. If alternatively the $J=2\rightarrow1$ line is considered displaced in frequency, as shown in Fig. 1, it is not possible to synthesize LVG line strengths consistent with observations. It may also be noted that very similar observations are obtained for optically thick wing zones (White et al., 1981) in L 1551, and the analysis of the spike feature considered here is therefore also pertinent to these cases.

As a result of this analysis it seems probable that the wing component in L 1551 is a post-shock phenomenon, with the relatively high temperatures representing some remnant of post-shock heating. The apparent presence however of large velocity gradients in the spike is rather surprising, since the spike feature appears to retain a more or less constant V_{LSR} over the entire dark cloud region, and is an obvious candidate for emission from the pre-shock zone. This may in turn imply that the current analysis is quite inadequate, and other contributions (from say turbulence) should be considered. Alternatively, one might suppose that the spike emission derives from a region which has undergone a previous compressive phase, perhaps originating from radiative acceleration of placental material into the more widespread cloud region. Further observations are required however before it will be possible to discriminate between these and other options.

We have further investigated the far-infrared continuum of IRS 5 and our results, together with those of Fridlund et al. (1980),

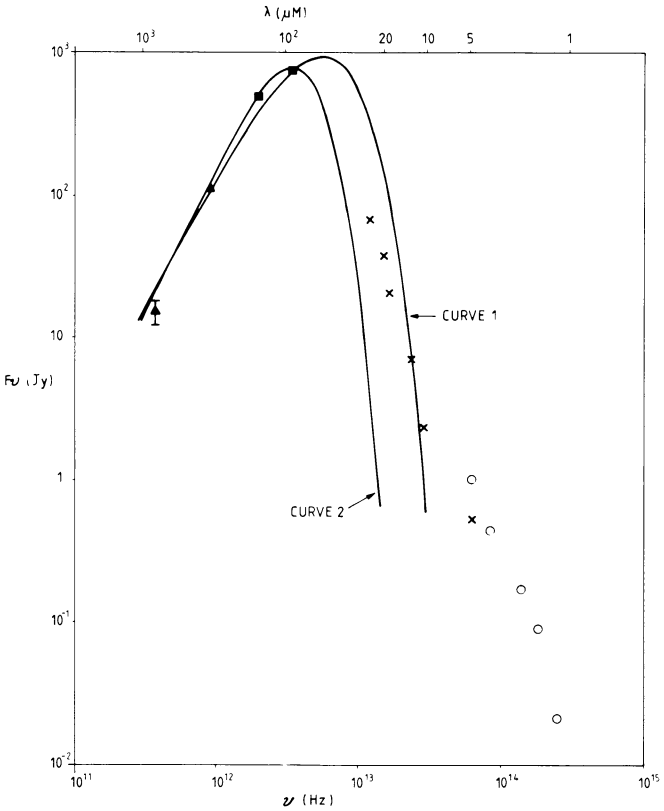

Fig. 3. The infrared continuum of IRS 5 in L 1551, with the present results (▲) complementing observations by Fridlund et al. (■), Beichman and Harris (×) and Strom, Strom and Vrba (○). Solid curves indicate solutions which are further discussed in the text

Beichman and Harris (1981), and Strom et al. (1976), are presented in Fig. 3. Measurements were also taken at the location of optically thin $J=3\rightarrow2$ CO results discussed earlier, resulting in a 2σ upper limit of 21.6 Jy at $\lambda=377\,\mu$m. This suggests that the central source measures in Fig. 3 are contaminated very little by emission from the dark cloud region.

Corresponding least-squares fits to the continuum have been attempted using the function:

$$F_\nu = WB_\nu(T)(1-e^{-\tau_\nu}),$$
$$\tau_\nu = \tau_0 \nu^\alpha,$$

where τ_ν is grain opacity (τ_0 is a constant), W is again dilution, and $B_\nu(T)$ the Planck function corresponding to temperature T. Two extreme cases are illustrated in Fig. 3; for Curve *1*, α is assumed to be small, and/or τ_0 large, with temperature taken as 95 K, i.e. the emission curve is that of a blackbody. For Curve *2*, τ_0 is assumed to be small, α is unity, and $T=40$ K, giving a variation $F_\nu \propto B_\nu(T)\nu$. The continuum observed longwards of 10 μm is seen to straddle these two extremes, and we find generally that no single temperature function of this kind can fully represent the data in this wavelength range, still less the short and long wavelength results combined.

It seems likely therefore that we must resort to models which take full account of radiative transfer effects and temperature variation through the cloud, in the manner of Scoville and Kwan (1976) and Tokunaga et al. (1978). For such cases, optical depth at the wavelength of peak emission is of order unity (Scoville and Kwan, 1976), and this would imply a relatively small source size at $\lambda\sim50\,\mu$m ($\sim2''$), increasing rapidly however to longer wavelengths where $\alpha\geqq1$. It is possible in consequence that the present results seriously underestimate F_ν at the longest wavelengths considered here, even allowing for present beam sizes.

Finally, we note that whilst no long-wave evidence is available for the size of IRS 5, the short wavelength emission clearly emanates from a warm, highly compact zone which may in turn be identifiable with the accretion disk hypothesized by Snell et al. (1980).

4. IRC+10 216

IRC+10 216 is a late type variable with moderate velocity gas outflow. The near-infrared spectrum appears to be composite, with evidence for optically thin SiC grain emission at wavelengths $\lambda\sim10\,\mu$m (cf. Treffers and Cohen, 1974).

The shorter wavelength ($\lambda\lesssim5\,\mu$m) continuum mimics a ~650 K black-body curve (cf. Becklin et al., 1969) but shows evidence for being highly polarised (Shawl and Sellner, 1970; Dyck et al., 1971; Capps and Knacke, 1976), and has been argued in consequence to represent scattering of the central star continuum (cf. Fazio et al., 1980).

Where source structure has been measured at wavelengths $\lambda\leqq11\,\mu$m, it appears to consist of two components: a small high temperature core, and a very much broader enveloping or "halo" zone. At $\lambda=11\,\mu$m this core is of size $<0''.2$, and is thought to represent the central star (Sutton et al., 1979); an 1800 K blackbody representing this component has been indicated in Fig. 5.

Far-infrared photometry of this source at λ377 μm, 811 μm, and 1136 μm is presented in Fig. 4, together with previously published infrared data. Apart from a discrepancy at $\lambda\sim350\,\mu$m between the present results and those of Campbell et al. (1976) (largely attributable to differing beam sizes), the present data is consistent with previous trends, and indicates a continuum falling as $F_\nu \propto \nu^{2.7}$. We have attempted to model this behaviour in terms of an optically thin grain distribution, and in accordance with the prescription of Fazio et al. (1980). This latter model assumes envelope density to fall with radius as:

$$\varrho(r)\propto\left\{1+\frac{r}{25''}\right\}/r^2 \tag{3}$$

a function principally determined from $J=2\rightarrow1$ CO mapping (Wannier et al., 1979). In addition however we assume a constant beam size $B=86''$ (within ~15% of all but one of the beams used in the acquisition of the submillimetre data in Fig. 4), and a grain temperature:

$$T_{gr}=T_0\left(\frac{r}{1''}\right)^{-\omega} \tag{4}$$

appropriate for an r^{-2} grain heating function, where $\omega=2/(4+\zeta)$, ζ is defined through the grain emissivity law $\varepsilon\propto\lambda^{-\zeta}$, and T_0 is a variable fitting parameter.

The best least-squares curve was obtained for $T_0\simeq230$ K, $\zeta=1$, and the fit is seen to be excellent, providing a strong indication that overall envelope properties are well represented by such a model. The internal radius was taken to be $r\sim0''.074$ corresponding to a maximum temperature $T=650$ K and it is clear from the modelling that the near-infrared continuum may also be readily synthesized. The level of the direct contribution of this

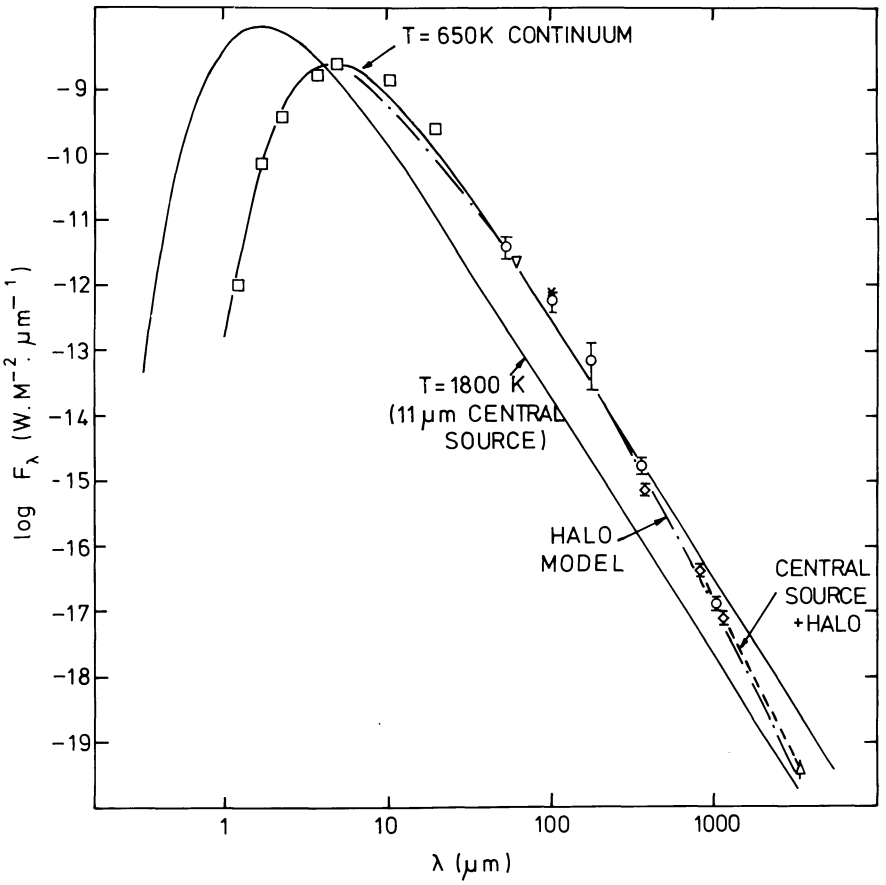

Fig. 4. The infrared continuum of IRC +10 216. □ Becklin et al. (1968) [as recalibrated by Toombs et al. (1972)]; ▽ Fazio et al. (1980); ○ Campbell et al. (1976) (as recalibrated by Fazio et al.); △ Schwatz and Spencer (1977); ◇ Present results; × Shivanandan et al. (1977). The 1800 K continuum is based on the discussion of Sutton et al. (1979), and models the central star continuum

emission to the observed continuum at these short wavelengths is difficult to gauge precisely because of the variable nature of the central star, a problem which also besets attempts to determine the integrated continuum energy (see later). Whilst these problems will ultimately require co-temporal near- and far-infrared measures before they can be properly overcome, it is possible to determine that at least a substantial fraction of near infrared flux may originate from the internal dust shell, rather than the central star. This radiation is then scattered by dust at larger radii to produce both the high levels of polarisation, and enhanced source radius (see later).

In adopting $\zeta = 1$ we follow the lead of Campbell et al., although their revised data (Fazio et al., 1980) would suggest a value $\zeta \simeq 0.7$ to be more appropriate. In both cases ζ is assessed from the slope of the observed continuum, a procedure which is strictly applicable only where the emission region has uniform temperature, and is entirely optically thin.

A potentially more sensitive way of evaluating ζ is to determine the trend of source FWHM (σ) with wavelength. For centrally heated envelopes in which grain density decreases with increasing radius, σ may be shown to vary as $\sigma \propto \lambda^{1/\omega}$, a result which is relatively insensitive to the precise details of envelope structure (Phillips and Beckman, 1980). Unfortunately, data concerning the size of IRC + 10 216 shows significant omissions at longer wavelengths, and our own attempts to fill this gap (at $\lambda \sim 35$ μm) were compromised by short-wavelength filter leaks. Scan profiles at $\lambda = 20$ μm with a 6″ beam indicated very little broadening over and above that expected for a point source, a result which is at least not inconsistent with the model, which predicts a source size $\sigma \sim 3\overset{''}{.}8$ and a FWHM after convolution with the beam of just $7\overset{''}{.}1$. Despite these deficiencies, the available long-wave data appears to imply a value $\zeta \cong 1$ (Fig. 5), and in this respect provides further support for the underlying assumptions of our model. In the short wavelength ($\lambda \lesssim 5$ μm) scattering regime, σ in contrast appears to asymptotically approach a value slightly in excess of $\sim 0\overset{''}{.}3$.

A further examination of envelope structure is possible through $J = 3 \rightarrow 2$ CO line profiles, and our results are presented in Fig. 6. Previous measures by Kuiper et al. (1976) in the $J = 1 \rightarrow 0$ CO transition showed a parabolic line profile indicative of constant velocity mass outflow, and these results were well modelled in terms of a constant temperature envelope. Subsequent $J = 2 \rightarrow 1$ mapping (Wannier et al., 1979) showed, however, a broad and roughly Gaussian variation of T_A^* on the sky – and indicated a size at variance with that expected for the constant mass-loss rate model of Kwan and Hill (1977). This result has been interpreted as indicating a secular decrease in dM/dt, and is the principal "raison d'être" of Eq. (3). On the basis of this analysis, we have assumed T_A^* to vary as

$$T_A^*(J = 2 \rightarrow 1) = T_{\max}(J = 2 \rightarrow 1)\, e^{-4 \ln 2 (r/\theta)^2} \qquad (5)$$

in modelling the $J = 3 \rightarrow 2$ spectrum, which thereby takes the form of a further test of the $T_A^*(J = 2 \rightarrow 1)$ mapping. The FWHM of this source is given by $\theta \simeq 37''$, and a value $T_{\max}(J = 2 \rightarrow 1) = 30$ K is adopted. For these circumstances the variation of $T_A^*(J = 3 \rightarrow 2)$ with radial velocity V is given (for constant outflow velocity) by Kuiper et al. (1976):

$$T_A^*(J = 3 \rightarrow 2, V) = T_{\max}(J = 3 \rightarrow 2)(1 + (B/\theta)^2 (1 - (V/V_0)^2)^{-1})^{-1} \qquad (6)$$

for optically thick lines. The parameter V_0 is a constant, and corresponds to the maximum observed radial velocity. This function is compared to our observed line profile in Fig. 6, and is

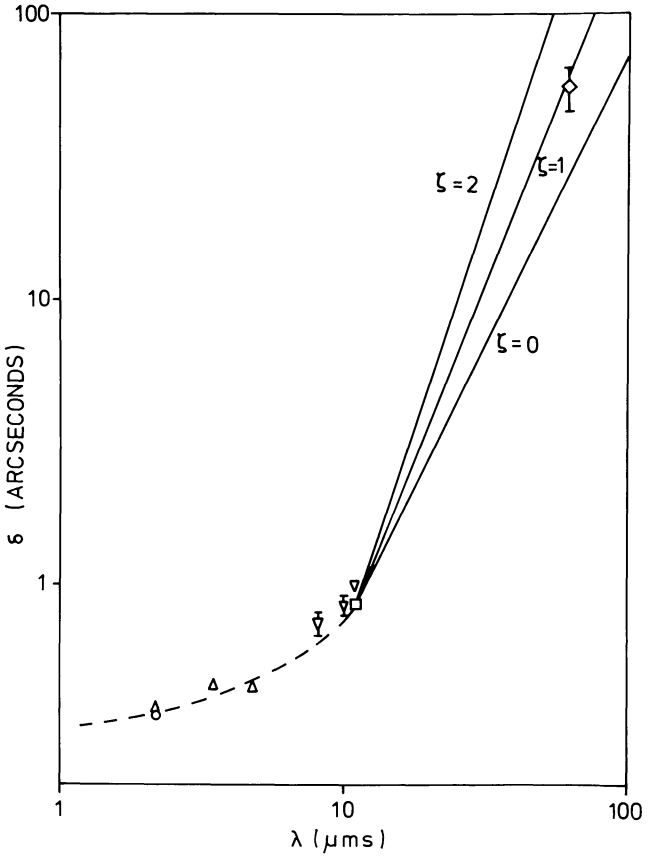

Fig. 5. The variation of source size with wavelength for IRC +10 216. △ Toombs et al. (1972); ○ Selby et al. (1979); □ Sutton et al. (1979); ◇ Fazio et al. (1980); ▽ Mc Carthy et al. (1977). The result of McCarthy and Low (1975) at $\lambda = 5$ μm is very similar to that of Toombs et al. at $\lambda = 4.8$ μm, and has been deleted for sake of clarity. The points of McCarthy et al. and Toombs et al. assume a disk-like source. Other measures are based on a Gaussian source shape. The three solid lines correspond to trends expected for three values of the emissivity exponent ζ

seen to give a reasonably good fit considering the noise. The present results therefore largely confirm lower frequency measures, and give some confidence that the source structure in CO is tolerably well established.

Finally, the far-infrared results may be combined with near infrared data (Fig. 4) to obtain a total continuum flux (with a proviso noted earlier concerning the variable nature of the central star). Temporarily placing aside the "excess" measurements at $\lambda\lambda$10 μm and 20 μm, we find total thermal emission + scattering to represent just 85% of the 1800 K central star flux. A proportion of the residual energy will also be radiated as "excess' emission in the near-infrared, through SiC bending modes. The correspondence between these two energy integrals is therefore as good as may be expected considering the uncertainties, and suggests that the 1800 K continuum in Fig. 4 is unlikely to deviate severely from the actual central star flux.

5. Conclusions

We have observed two stellar sources associated with high mass-loss rate outflows, at millimetre and submillimetre wavelengths.

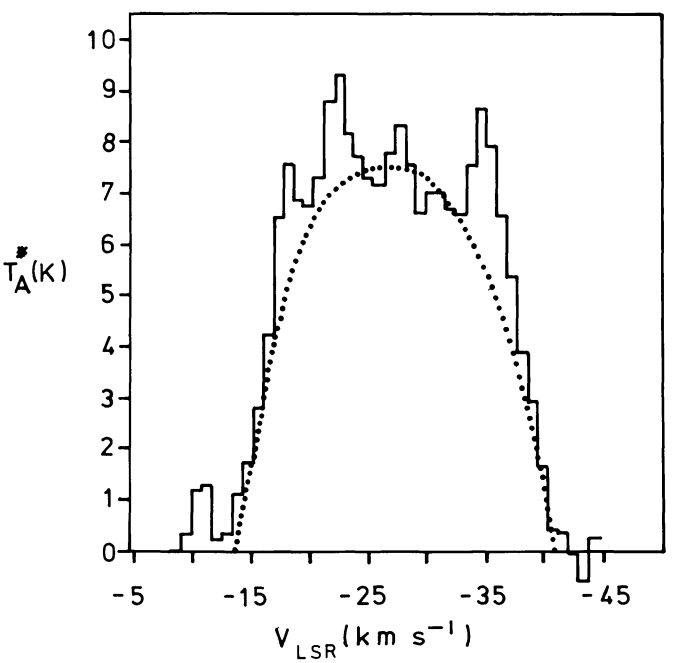

Fig. 6. $J = 3 \rightarrow 2$ CO spectrum of IRC + 10 216, with comparison model profile (see text)

L 1551 appears to locate a region where a high velocity stellar wind is interacting with a dark cloud, and our results show the presence of strong velocity gradients in the (presumed) pre- and post-shock components, together with moderately high temperatures and densities. Far-infrared measurements enable the continuum to be extended for the first time into the Rayleigh-Jeans limit, and indicate that modelling of this source will require an emission continuum corresponding to a range of grain temperatures. We have also obtained a spectrum for IRC + 10 216 in the $J = 3 \rightarrow 2$ line of CO, together with photometry at wavelengths 377 μm, 811 μm, and 1136 μm. The convolution of our beam profile with the $J = 2 \rightarrow 1$ temperature distribution (suitably scaled for the higher frequency) enables adequate fits to the $J = 3 \rightarrow 2$ data, and the far-infrared measures have also been modelled reasonably well in terms of a distribution of optically thin grains, with emissivity varying as $\varepsilon \propto \lambda^{-1}$. The change of source FWHM σ with wavelength predicted by this model appears to be consistent with observations, although further confirmatory measures at $\lambda \sim 35$ μm (where it is to be expected that $\sigma \sim 15''$) would be of considerable interest.

Acknowledgements. We thank Mr. D. W. Walker for helpful discussions, Drs. Bill Zealey and Andy Longmore for night assisting, the staff of UKIRT for operation of UKIRT, PATT for the award of telescope time, and the SRC for travel funds and support and funding of the millimetre/submillimetre wave astronomy and receiver development at QMC. JPP thanks ESA for a research fellowship.

References

Becklin, E.E., Frogel, J.A., Hyland, A.R., Kristian, J., Neugebauer, G.: 1969, *Astrophys. J.* **158**, L133
Beichman, C., Harris, S.: 1981, *Astrophys. J.* **245**, 589

Campbell, M.F., Elias, J.H., Gezari, D.Y., Harvey, P.M., Hoffmann, W.F., Hudson, H.S., Neugebauer, G., Soifer, B.T., Werner, M.W., Westbrook, W.E.: 1976, *Astrophys. J.* **208**, 396

Capps, R.W., Knacke, R.F.: 1976, *Publ. Astron. Soc. Pacific* **88**, 224

Clark, F.O., Biretta, J.A., Martin, H.M.: 1979, *Astrophys. J.* **234**, 922

Cunningham, C.T., Ade, P.A.R., Robson, E.I., Nolt, I.G., Radostitz, J.V.: 1981, *Icarus* (in press)

Dyck, H.M., Forbes, F.F., Shawl, S.J.: 1971, *Astrophys. J.* **76**, 901

Fazio, G.G., McBreen, B., Stier, M.T., Wright, E.L.: 1980, *Astrophys. J.* **237**, L39

Fridlund, C.V.M., Nordh, H.L., van Duinen, R.J., Aalders, J.W.G., Sargent, A.I.: 1980, *Astron. Astrophys.* **91**, L1

Goldreich, P., Kwan, J.: 1974, *Astrophys. J.* **189**, 441

Green, S., Thaddeus, P.: 1974, *Astrophys. J.* **191**, 653

Knapp, G.R., Kuiper, T.B.H., Knapp, S.L., Brown, R.L.: 1976, *Astrophys. J.* **206**, 443

Kuiper, T.B.H., Knapp, G.R., Knapp, S.L., Brown, R.L.: 1976, *Astrophys. J.* **204**, 408

Kwan, J., Hill, F.: 1977, *Astrophys. J.* **215**, 781

McCarthy, D.W., Low, F.J.: 1975, *Astrophys. J.* **203**, L37

McCarthy, D.W., Low, F.J., Howell, R.: 1977, *Astrophys. J.* **214**, L85

Phillips, J.P., Beckman, J.E.: 1980, *Monthly Notices Roy. Astron. Soc.* **193**, 245

Robson, E.I., Eve, W.D., Ade, P.A.R., Rice, D.P., Clegg, P.E., El-Atawy, S.: 1978, *Infrared Phys.* **18**, 781

Schwartz, P.R., Spencer, J.H.: 1977, *Monthly Notices Roy. Astron. Soc.* **180**, 297

Scoville, N.Z., Kwan, J.: 1976, *Astrophys. J.* **206**, 718

Selby, M.J., Wade, R., Sanchez Magro, C.: 1979, *Monthly Notices Roy. Astron. Soc.* **187**, 553

Shawl, S.J., Sellner, B.: 1970, *Astrophys. J.* **162**, L19

Shivanandan, K., McNutt, D.P., Daehler, M., Moore, W.J.: 1977, *Nature* **265**, 513

Snell, R.L., Loren, R.B., Plambeck, R.L.: 1980, *Astrophys. J.* **239**, L17

Strom, K.M., Strom, S.E., Vrba, F.J.: 1976, *Astrophys. J.* **81**, 320

Sutton, E.C., Betz, A.L., Storey, J.W.G., Spears, D.L.: 1979, *Astrophys. J.* **230**, L105

Tokunaga, A.T., Erickson, E.F., Caroff, L.J., Dana, R.A.: 1978, *Astrophys. J.* **224**, L19

Toombs, R.I., Becklin, E.E., Frogel, J.A., Low, S.K., Porter, F.C., Westphal, J.A.: 1972, *Astrophys. J.* **173**, L71

Treffers, R., Cohen, M.: 1974, *Astrophys. J.* **188**, 545

Wannier, P.G., Leighton, R.B., Knapp, G.R., Redman, R.O., Phillips, T.G., Huggins, P.J.: 1979, *Astrophys. J.* **230**, 149

Wannier, P.G., Redman, R.O., Phillips, T.G., Leighton, R.B., Knapp, G.R., Huggins, P.J.: 1979, IAU *Symp.* **87**, ed. B. H. Andrew, Reidel, Dordrecht, Holland, p. 487

White, G.J., Watt, G.D., Cronin, N.J., van Vliet, A.H.E.: 1979, *Monthly Notices Roy Astron. Soc.* **186**, 107

White, G.J., Phillips, J.P., 1981, *Monthly Notices Roy. Astron. Soc.* **194**, 947

White, G.J., Phillips, J.P., Watt, G.D.: 1981, *Monthly Notices Roy. Astron. Soc.* **197**, 745

Wright, E.L.: 1976, *Astrophys. J.* **210**, 250